runs taken on the 8 × 16 particle size. It can be seen that x_{H_2} becomes zero around a gas concentration of 4 mole % methane. In other words when concentration of 4 mole % methane is reached on the breakthrough curve, no hydrogen remains adsorbed on the bed. For the other particle sizes x_{H_2} becomes zero at roughly the same concentration.

After the zero was dropped, x_{H_2} did not remain constant but became slightly positive for some of the runs. This deviation was most serious for the high flow rate runs because the slopes of the curves used to find $(\partial q/\partial t)_z$ were steepest in these cases and therefore less precise.

Another reason for this deviation may be that the experimentally measured temperature lagged behind the true bed temperature toward the end of a run. If one considers Equation (5), it can be seen that if the true temperature is lower than that measured q^* will be higher, and in turn x_{H_2} will be lower.

SUMMARY

A rate equation is presented which describes data obtained on the adsorption of methane from hydrogen by silica gel. The bed temperature has been used and the adsorption rates have been calculated without making the usual simplifying assumption. The particle transfer coefficient is dependent on flow rate, and the quantity x_{H_2} seems to have a definite relationship with gas concentration.

The model has been applied to a system with a linear equilibrium adsorption isotherm in this paper and in a previous work (*1*) to a system with a favorable equilibrium or constant pattern. In view of these facts the utility of this model is felt to be demonstrated.

ACKNOWLEDGMENT

This research was supported by a grant from the Petroleum Research Fund administered by the American Chemical Society. Grateful acknowledgment is hereby made to the donors of this fund.

NOTATION

A = cross-sectional area of bed, sq. ft.
C = concentration of adsorbate in fluid phase, mole/cu. ft.
C^* = interface gas concentration, mole/cu. ft.
F = volumetric flow rate, cu. ft./min.
K_p = particle transfer coefficient, 1/min.
M = molecular weight
p = partial pressure of methane in gas stream, atm.
p^* = interface partial pressure of methane, atm.
q = average adsorbate concentration in particle, lb. adsorbate/lb. adsorbent
q^* = adsorbate concentration of particle at interface, lb. adsorbate/lb. adsorbent
q_∞ = adsorbate concentration in equilibrium with C_∞, lb adsorbate/lb. adsorbent
Q_∞ = $(1 - x_{H_2})\, q_\infty$
t = time, min.
T = temperature
x_{H_2} = $(q/q_\infty)_{H_2}$
z = bed length
ϵ = bed porosity, cu. ft. void/cu. ft. bed
ρ_B = bulk density, lb. adsorbent/cu. ft. bed

LITERATURE CITED

1. Geser, J. J., Ph.D. dissertation, Carnegie Inst. Technol., Pittsburgh, Pennsylvania (1961).
2. Glueckauf, E., *Trans. Faraday Soc.*, **51**, 1540 (1955).
3. Hiester, N. K., et al., *A.I.Ch.E. Journal*, **2**, 404 (1956).
4. Hiester, N. K., and Theodore Vermeulen, *Chem. Eng. Progr.*, **48**, 505 (1952).
5. Hougen, O. A., and K. W. Watson, "Chemical Process Principles," Part 3, p. 987, Wiley, New York (1947).
6. Moison, R. L., and H. A. O'Hearn, Jr., *Chem. Eng. Progr. Symposium Ser. No. 24*, **55**, 71 (1959).
7. Thomas, H. C., *J. Am. Chem. Soc.*, **66**, 1664 (1944).
8. ———, *Ann. N. Y. Acad. Sci.*, **49**, 161 (1948).

Manuscript received October 13, 1961; revision received February 5, 1962; paper accepted February 6, 1962. Paper presented at A.I.Ch.E. Los Angeles meeting.

Heat Transfer from a Cylinder to a Power-Law Non-Newtonian Fluid

M. J. SHAH, E. E. PETERSEN, and ANDREAS ACRIVOS

University of California, Berkeley, California

For low-molecular-weight liquids and for all gases it has been postulated and repeatedly verified experimentally that the shear stress imposed on the fluid is directly proportional to the rate of strain at constant temperature and pressure. The proportionality constant in this linear relation is called the *viscosity* and for the simple one-dimensional flow is defined by

$$\mu = \frac{\tau}{du/dy} \qquad (1)$$

It is found however that for many fluids—solutions of organic macromolecules, pulps, slurries, molten plastics, etc.—the viscosity coefficient in Equation (1), instead of being only a property of the material and thus independent of its state of motion, is also markedly affected by changes in the shear rate. It is clear therefore that for such rheological substances, which are grouped together under the common name *non-Newtonian fluids*, the concept of viscosity is a rather useless one and that an expression different from Equation (1) must be sought to relate the local stress to the hydrodynamic variables of the system.

In the past various models relating shear rate and shear stress have been proposed for different types of non-Newtonian behavior (*7*). Among the more commonly encountered expressions are those for Bingham plastic fluids, for which

$$\tau - \tau_y = \eta \left(\frac{du}{dy}\right) \qquad (2)$$

and those for power-law fluids, where, again for one-dimensional flow conditions

$$\tau = K \left(\frac{du}{dy}\right)^n \qquad (3)$$

with $n < 1.0$ for pseudoplastics and $n > 1.0$ for dilatant substances.

The functional relation between the stress and the state of motion of the fluid, the so-called *rheological equation of state*, must as a rule be obtained experimentally. Even so, the interpretation of the experimental results is seldom unequivocal because in general the stress is a function not only of the rate of strain, but also of the higher

M. J. Shah is with International Business Machines Corporation, San Jose, California. Andreas Acrivos is at Stanford University, Stanford, California.

spatial derivatives of the velocity components and the various components of the local acceleration (*9, 10*). Yet it has been shown that measurements with standard viscometers, such as the rotating cup or the capillary tube, do not always correctly lead to the complete rheological equation of state, and sometimes even fail to detect part of the terms. It is known for example that it is impossible to predict, on the basis of the capillary tube viscometer data alone, whether or not the fluid will show viscoelastic properties or exhibit the rather striking Weissenberg (*13*) and Merrington (*6*) effects. Similarly, although it invariably becomes necessary to postulate the existence of complete isotropy in the flowing medium, the solid surface does bring about a preferred orientation in the field of motion, and the resulting anisotropy may under certain circumstances be an important factor. It is plausible to suppose then that although a rheological equation of state, as obtained experimentally from standard viscometer measurements, may be adequate for certain hydrodynamic conditions, it does not necessarily mean that it will also correctly represent the state of stress of the system for geometrical flow configurations which are appreciably different from those on which the rheological experiments were originally performed.

The present investigation was therefore undertaken to probe this rather interesting question in some detail. A dilute solution of carboxymethylcellulose in water, the rheological properties of which were first determined in a standard capillary tube viscometer, was recirculated in a closed-circuit water tunnel in which a uniformly heated cylinder was placed with its axis normal to the flow. The experiments were carried out under the laminar boundary-layer type of flow conditions, which are different in character from the state of motion existing in the capillary tube and yet are simple enough to permit a theoretical analysis. The investigation was restricted to those carboxymethylcellulose solutions which were found to follow the power law and which to all appearances did not show any viscoelastic effects. The purpose of this work was then to compare the experimentally measured temperature distribution on the surface of the cylinder with the results of a theoretical analysis which contained no adjustable parameters and which required for each fluid only the independent evaluation of the rheological constants K and n appearing in Equation (3).

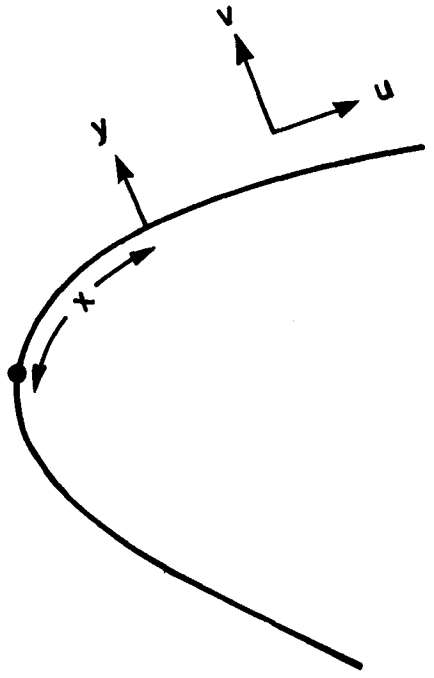

Fig. 1. Showing the directions of the coordinates x and y and the velocities u and v with respect to the surface.

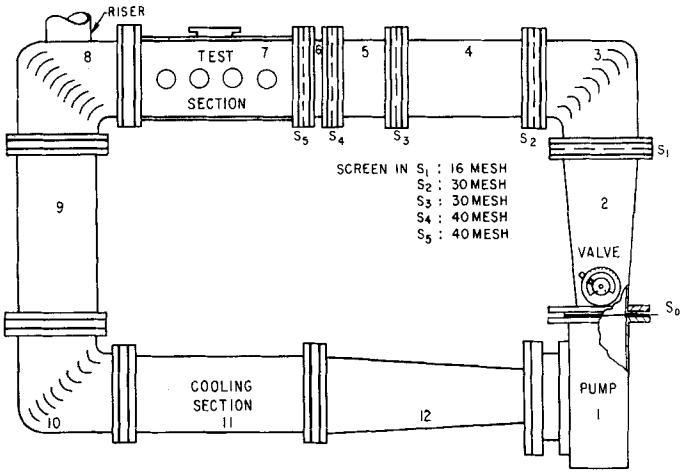

Fig. 2. The water tunnel.

THEORETICAL ANALYSIS

It has already been shown in an earlier communication (*2*) that the well-known laminar boundary-layer equations of Newtonian hydrodynamics may easily be extended to include power-law fluids. Thus for the smooth but otherwise arbitrary two-dimensional surface of Figure 1

$$u_1\frac{\partial u_1}{\partial x_1}+v_1\frac{\partial u_1}{\partial y_1}=\Phi(x_1)\frac{d\Phi}{dx_1}+\frac{\partial}{\partial y_1}\left(\frac{\partial u_1}{\partial y_1}\right)^n \quad \text{(equation of motion)} \quad (4)$$

$$\frac{\partial u_1}{\partial x_1}+\frac{\partial v_1}{\partial y_1}=0 \quad \text{(equation of continuity)} \quad (5)$$

$$u_1\frac{\partial T}{\partial x_1}+v_1\frac{\partial T}{\partial y_1}=\frac{1}{N_{Pr}}\frac{\partial^2 T}{\partial y_1^2} \quad \text{(heat convection equation)} \quad (6)$$

where

$$x_1=\frac{x}{L},\quad u_1=\frac{u}{U_c},\quad \Phi(x_1)=\frac{U_i}{U_c},$$

$$v_1=N_{Re}^{\frac{1}{1+n}}\frac{v}{U_c},\quad y_1=N_{Re}^{\frac{1}{1+n}}\frac{y}{L},$$

$$N_{Re}\equiv\frac{\rho U_c^{2-n}L^n}{K},$$

$$N_{Pr}=\frac{c_p U_c \rho L}{k}(N_{Re})^{-\frac{2}{1+n}}$$

where, in accordance with the boundary-layer theory, $\Phi(x_1)$ is uniquely determined by the geometry of the surface and is the same for both Newtonian and non-Newtonian substances.

The solution to Equations (4) to (6), which are the correct asymptotic forms of the exact equations of motion, continuity, and energy if $N_{Re} >> 1$ and if the dissipation term in the heat-convection equation is neglected, must also satisfy the usual boundary conditions:

$$\begin{aligned} &y_1=0;\quad u_1=v_1=0;\quad T=T_s(x_1)\\ &x_1=0 \text{ and } y_1=\infty;\quad u_1=\Phi(x_1);\quad T=T_\infty \end{aligned} \quad (7)$$

where for the moment the surface temperature has been left as an unspecified function of the boundary-layer coordinate x_1.

As might be suspected, the exact solution of Equations (4) to (7) is in the general case a problem of considerable difficulty which fortunately can in most instances be solved by an approximate, but quite accurate, technique. This is so because for the large majority of power-law fluids the generalized Prandtl number is large, which means (*8*) that Equation (6) may be simplified into its asymptotic form for $N_{Pr}\to\infty$:

$$\lambda(x_1)\,y_1\frac{\partial T}{\partial x_1}-\frac{y_1^2}{2}\frac{d\lambda}{dx_1}\frac{\partial T}{\partial y_1}=\frac{1}{N_{Pr}}\frac{\partial^2 T}{\partial y_1^2} \quad (8)$$

$$\lambda(x_1) \cong \left[\sum_{i=1}^{j} \alpha_i x_i^{\frac{6m_i-2}{3}}\left\{(1-m_i+2m_in)\,[g_n]^{n+1}+\frac{2m_i(n+1)}{3n}\right\}^{2/3}\right]^{\frac{3}{2(n+1)}} \quad (13)$$

where

$$\lambda(x_1) \equiv \left(\frac{\partial u_1}{\partial y_1}\right)_{y_1=0}$$

It can now be shown (3, 5) that

$$-\left(\frac{\partial T}{\partial y_1}\right)_{y_1=0} = \left(\frac{N_{Pr}}{9}\right)^{1/3} \frac{\sqrt{\lambda}}{\Gamma(4/3)} \int_0^{x_1} \frac{dT_s(z)}{\left[\int_z^{x_1} \sqrt{\lambda}\, d\xi\right]^{1/3}} \quad (9)$$

with $T_s = T_\infty$ as $x_1 \to 0$, which, as first pointed out by Lighthill (5), provides usually an excellent approximation to the exact solution even when N_{Pr} is as low as 10. Equation (9) may finally be rearranged by a standard Laplace transformation into

$$T_s - T_\infty = -\frac{\Gamma(4/3)}{\Gamma(2/3)\,\Gamma(1/3)} \left(\frac{9}{N_{Pr}}\right)^{1/3} \int_0^{x_1} \left(\frac{\partial T}{\partial y_1}\right)_{y_1=0} \left[\int_z^{x_1} \sqrt{\lambda}\, d\xi\right]^{-2/3} dz \quad (10)$$

which is more convenient since the experiments were carried out under constant flux conditions. If in particular

$$Q = -kA\left(\frac{\partial T}{\partial y}\right)_{y=0} = -\frac{kA}{L}(N_{Re})^{-\frac{1}{1+n}}\left(\frac{\partial T}{\partial y_1}\right)_{y_1=0}$$

then Equation (10) may be simplified still further into

$$N_{Nu} \equiv \frac{QL}{Ak}\frac{1}{T_s - T_\infty} = \frac{\Gamma(1/3)\,\Gamma(2/3)}{\Gamma(4/3)} N_{Re}^{\frac{1}{1+n}} \left(\frac{N_{Pr}}{9}\right)^{1/3} \left\{\int_0^{x_1}\left[\int_z^{x_1} \sqrt{\lambda}\, d\xi\right]^{-2/3} dz\right\}^{-1} \quad (11)$$

It remains now to show how the function $\lambda(x_1)$ is to be determined from Equations (4) and (5). Again, although an exact solution cannot be obtained in the general case, except by a laborious finite-difference numerical procedure, an approximate but accurate expression for $\lambda(x_1)$ can be devised. The details, which are presented elsewhere (*11*), are omitted here; the final result is as follows.

If it is supposed that $\Phi^2(x_1)$ is expanded in the form

$$\Phi^2(x_1) = \sum_{i=1}^{j} \alpha_i x_1^{2m_i} \quad (12)$$

where the coefficients α_i and m_i can easily be calculated by a straightforward least-squares procedure, as originally developed in connection with Prony's interpolation formula (*14*). Of course the exponents $2m_i$ need not be integers. Then by a straightforward extension of an earlier expression (1), which at the time was derived for Newtonian fluids only

where the function $[g_n]^{n+1}$ is given in Table 1.

One can see from Equations (11) to (13) therefore that once the rheological parameters K and n of the fluid have been independently determined, the calculation of the local surface temperature for a given rate of heat input can easily be carried out if the pressure distribution around the body is available either from a theoretical potential flow model or from experimental measurements. It is especially important to realize however that Equation (11) contains no arbitrary constants. This would imply that agreement between the predictions of the theoretical analysis and the experimental data should be interpreted as strongly indicating that, in the absence of viscoelastic effects, a rheological equation of state derived from standard viscosity measurements can still be retained to describe the stress rate of strain relation for flow conditions of the laminar boundary-layer type.

EXPERIMENTAL APPARATUS

The major items of the experiment station were (a) a water tunnel with a pump, screens, vanes, a valve, and a cooling system; (b) a test section and cylinders for heat transfer and pressure measurements; (c) a pressure-and velocity-measurement assembly; (d) an electrical power supply and measurement system; and (e) a capillary viscometer.

Water Tunnel and Its Accessories

The water tunnel is in many respects similar to the one described by Kiser (*4*). As shown in Figure 2 it consists of twelve different sections which, with the exception of sections 1 and 7, were constructed from 1/16-in. thick type-304 stainless steel sheets. The sheets were welded to form 8 by 10 in. rectangular sections, held together by stainless steel flanges with Plexiglas frames between them. Stainless steel screens were cemented in the Plexiglas frames S_1, S_2, S_3, S_4, and S_5, and the fluid was passed successively through smaller screens as it approached the test section. The function of the screens was to dampen out the turbulent velocity fluctuations of the main stream. In addition a 40-mesh screen welded in a stainless steel frame S_0 was placed at the exit flange of the pump to collect any extraneous solid particles which could clog the other screens.

The fluid was circulated by a cast-iron centrifugal pump having a capacity of 1,400 gal./min. of water at a head of 6 ft. The inside body of the pump and the impeller surface were coated with an epoxy resin to protect the iron surfaces from the carboxymethylcellulose solutions.

In the corner sections, 3, 8, and 10, a row of vanes was welded across to guide the fluid around the bends with minimum losses. Sections 4, 5, and 6 acted more or less as calming sections between screens. The turbulence was expected to decay completely at about a distance of 10 to 30 mesh lengths downstream from the last screen, 4.

The test section, 7, was made from ¾ in.-thick Plexiglas and, in order to improve the strength of the plastic, was mounted with long steel studs going from flange to flange. The four holes in this section, seen in the figure, were 2 in. in diameter and supported the test piece, its accessories, and the pitot tube. The valve for regulating the fluid circulation rate consisted mainly of two sets of bars bent from 1/16 in. thick stainless steel sheets to form a triangular cross section where one set would fit into the other. The movement of the central shaft rotated the cam mounted on it, which in turn pushed the inner frame down, thus closing the gaps between the sets of bars. The valve could be set in such a way that velocities as low as 1 ft./sec. were produced in the test section.

The heat generated in the fluid by recirculation was unfortunately quite appreciable (15,000 to 20,000 B.t.u./hr.) and had to be removed by means of a refrigeration unit which was placed in section 11 of the tunnel. An auxiliary water cooler was added later to increase the capacity of the condenser.

Test Pieces

The pressure measurements were carried out with a 2 in. diameter aluminum cylinder 9-½ in. long. The total pressure (dynamic and static) was read at a 1/16-in. hole drilled normal to the curved surface at a distance of 4-¾ in. frome one end. The fluid was led out by means of a ⅛-in. hole drilled from one end of the cylinder connecting the 1/16-in. hole. At the other end of the cylinder a protractor was mounted to measure the position of the pressure tap relative to the stagnation point. The cylinder was inserted in the third downstream aperture in the test section. The static pressure was measured by means of the static holes of a pitot tube, placed 4 in. ahead of the stagnation point of the cylinder. An approximate calculation indicated that the pressure drop in this 4-in. section due to the flow of the carboxymethylcellulose solutions in the tunnel was negligible.

The test piece that was used for the heat transfer measurements is shown in Figure 3. It was 2 in. in diameter and 9½ in. long and was made from fabric-base phenol-formaldehyde resin. It was heated by passing electric current through a series of twenty-six strips of Chromel A (No. 24), each of them 3/16 by 0.0201 in. by 4¾ in., with a resistance of 0.135 ohm/ft. The strips were mounted in grooves milled on the curved surface of the cylinder, 0.054-in. segments of resin being allowed between successive grooves. Since it was necessary to construct a smooth cylindrical heating surface having a 2-in. diameter, the Chromel strips were prebent to a 1-in. radius and cemented in the grooves. The diameter of the finished test piece was 2.0 ± 0.003 in. The strips were connected electrically in series by pieces of copper ribbons held in position by solder and screws. The strip ends were then covered

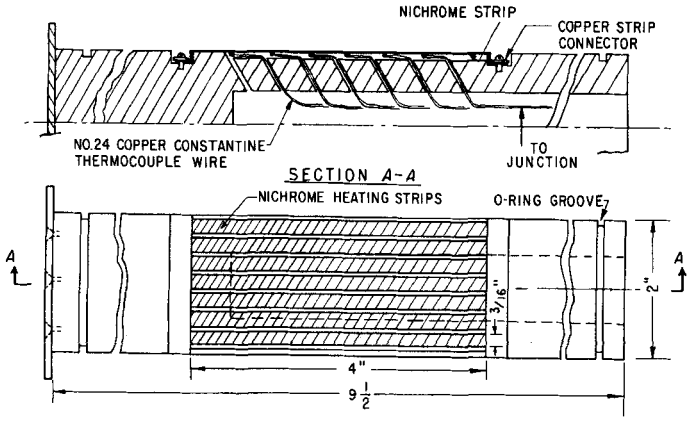

Fig. 3. Heat transfer cylinder.

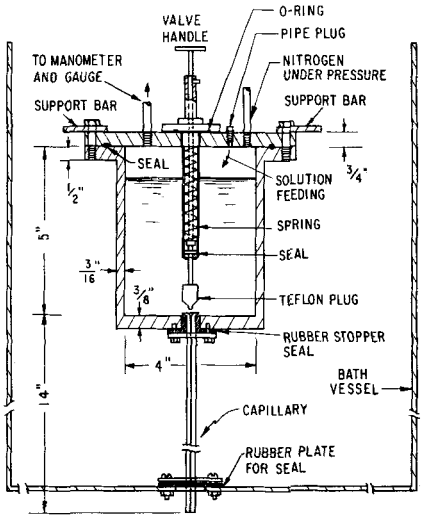

Fig. 4. The capillary viscometer.

with cement, and the surface was finished to 2.0 in. Surface temperatures were measured by means of six thermocouples spot welded onto its back face. As shown in Figure 3 the thermocouples were welded ½ in. apart and, in order to minimize losses due to conduction, were laid parallel to the strip before being led out through the resin. The six thermocouples, when calibrated in the constant-temperature bath, were found to read the same temperature within less than 0.2°F.

The thermocouple wires and the power lines were inserted through the ¾-in. hole in the cylinder at one end, and at the other end a protractor assembly similar to that of the pressure cylinder was attached.

During a heat transfer run air bubbles were observed collecting on the surface of the cylinder, thus insulating the surface and giving rise to errors in the temperature measurements. A wiper was used to remove these bubbles and to maintain a clean surface.

Pressure and Velocity Measurements

The pressure readings on the cylinder and the velocity measurements from a pitot tube were recorded by means of a water–carbon tetrachloride differential manometer. The pitot tube consisted of a ⅛ in. O.D. Dwyer tube with a 0.047-in. diameter dynamic hole and four equally spaced 0.04-in.-diameter apertures for static pressure measurements. Once the velocity measurements had been completed, the pitot tube was pulled close to the wall of the tunnel to prevent any disturbances on the temperature measurements.

In the preliminary velocity measurements with the carboxymethylcellulose solutions the manometer response was sluggish owing to the gel centers in the solutions supporting a shear in the pitot tube holes (*3a*). This difficulty was overcome by slowly bleeding the manometer leads with water and of course by stopping the bleeding just before a pressure measurement was taken.

Capillary Viscometer

A capillary type of viscometer was constructed according to the recommendations of Metzner (*7*) for determining the rheological characteristics of the carboxymethylcellulose solutions which were used in this investigation. As shown in Figure 4 the viscometer consisted of three major parts: a constant-temperature bath; a 1,000-ml. pressure vessel; and a set of precision-bore capillary tubes of different but constant diameters.

The pressure vessel was constructed from a 4-in. I.D. stainless steel pipe with a flange welded on one side, and the other side was sealed with a ¾ in. thick stainless steel piece. The vessel was also provided with a lid which had the necessary connections to the nitrogen line to the pressure manometer and pressure gauge and had a hole for feeding the solution. The lid was sealed by means of an O-ring.

The capillary tube was supported by a machined rubber stopper which in turn was held by a flange. The upper end of this tube was shaped to minimize the entrance losses and to form a seat for the Teflon bob of the spring-loaded valve. As shown in the figure, the valve was operated by a lever which pushed the spring pressure on the tube entrance.

Two capillary tubes, one of .40-in. O.D. and 14 in. long and the other .0707 in. I.D. and 12 in. long, were found most suitable for the carboxymethylcellulose solutions. The uniformity of their diameters was checked by measuring the dimensions of a small mercury column at different points along the entire length of the tube. The diameter variation was found to be less than 0.5%.

The pressure in the vessel was measured either by a carbon tetrachloride or a mercury manometer. The carboxymethylcellulose solution which emerged from the capillary tube was collected at the bottom of the bath and weighed on a balance with a precision of ±0.01 g.

RESULTS AND DISCUSSION

It has already been stated that the primary purpose of this investigation was to test the hypothesis that a rheological equation of state of a non-

Table 1. Function g_n for Different Values of n (2, 11)

n	g_n	$[g_n]^{n+1}$
0.05	1.49803	1.52860
0.1	0.80574	0.78852
0.2	0.48247	0.41703
0.3	0.38813	0.29219
0.5	0.33126	0.19066
1.0	0.33206	0.11026
1.5	0.36477	0.08036
2.0	0.39979	0.06390
2.5	0.43261	0.05325
3.0	0.46243	0.04573
4.0	0.510	0.03450
5.0	0.552	0.02829

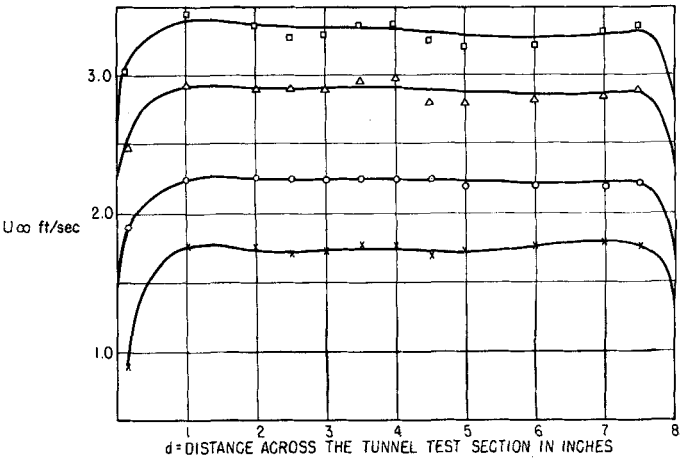

Fig. 5. Velocity profiles across the tunnel at 15 in. from the last screen.

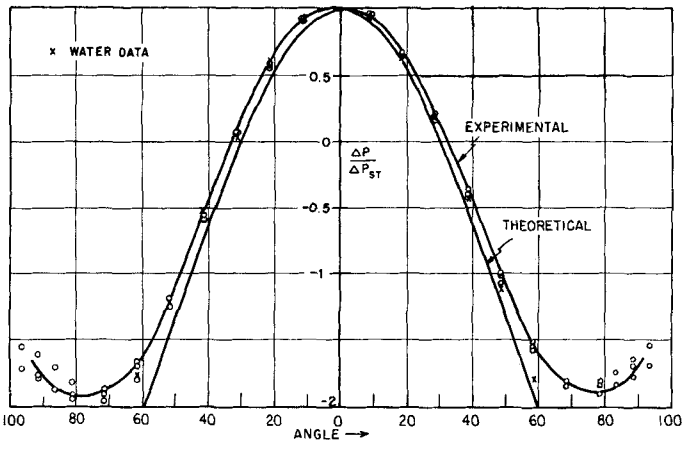

Fig. 6. Pressure distribution around the cylinder. Solution in the tunnel 0.221% carboxymethylcellulose.

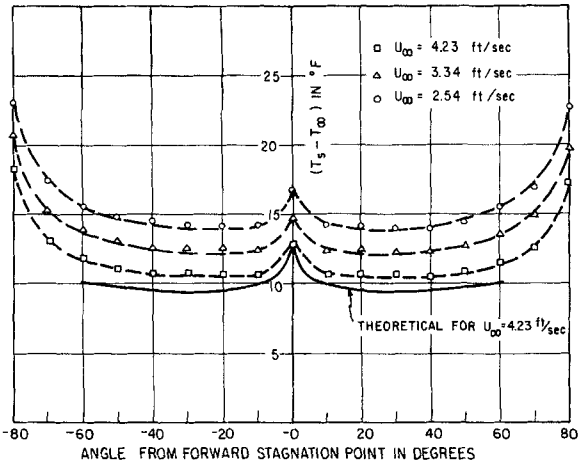

Fig. 8. Temperature distribution around the cylinder. Solution 0.09% carboxymethylcellulose 70S.

Newtonian fluid as derived experimentally from a standard viscometer may be used to predict the behavior of the fluid in laminar boundary-layer flows. The rheological constants for the carboxymethylcellulose solutions used here were therefore obtained by means of the capillary viscometer just described, whereas the pressure distribution and the rate of heat transfer from the electrically heated cylinder to the carboxymethylcellulose solutions in forced convection flows were determined in the tunnel assembly. It is understandable then that the applicability of the theoretical model which was developed in this paper will be judged principally by the degree of correspondence between the theoretically calculated and the measured surface temperature distributions.

It is clear of course that before a meaningful comparison can be made between the experimental results and those derived theoretically, it is important that the experimental setup fulfill as far as possible the restrictions which were imposed on the mathematical model. Otherwise the degree of correspondence between the theoretical and experimental results may be limited by an inability to meet these requirements in the physical system to be investigated. The three assumptions most pertinent to this discussion are:

1. The flow is truly two dimensional.
2. The rheological parameters K and n are constant over the range of shear rates on the surface, and that both the cross viscosity of the carboxymethylcellulose and any viscoelastic properties are negligible.
3. The cylinder is heated by a uniform flux source.

The first assumption can be verified by obtaining the velocity distribution in the test section of the tunnel. On the other hand it can easily be ascertained from the rheological data whether K and n will remain constant for all shear rates of interest, and it is a simple matter to modify the calculations if it is found that their values vary somewhat. The experimental setup does not however rigorously conform to the last requirement because the surface of the cylinder was heated with Chromel strips separated by insulating segments of phenol-formaldehyde resin. The heating of the cylinder surface was therefore not achieved by a truly uniform flux as required by the theoretical model. As a consequence, since the insulating segments covered a little over 20% of the total area, the experimental heat transfer coefficients would have to be lower than if the heating had been uniform, because the surface temperatures, which were measured along the center line of the Chromel strip, would under these circumstances be somewhat higher. Fortunately however a theoretical analysis of this effect (*11*) showed that it could cause only a relatively minor discrepancy which in general would not exceed 10%.

The measured velocity profiles across the test section of the tunnel are shown in Figure 5. It is seen that the screens insured fairly uniform velocities across the test section and that

Table 2. Rheological Properties of the Carboxy-Methyl Cellulose Solutions from the Plots of $\frac{D\Delta P}{4L}$ vs. $8V/D$

Concentration of CMC 70	Shear rate range $8V/D$, sec.$^{-1}$	K, lb.$_f$/sq. ft. $\cdot$ sec.^{n}	n
0.09%	1,000-30,000	0.92×10^{-3}	0.72
0.22%	10-900	1.7×10^{-3}	0.79
	900-10,000	6.3×10^{-3}	0.63
0.35%	100-900	5.4×10^{-3}	0.66
	900-10,000	8.8×10^{-3}	0.58

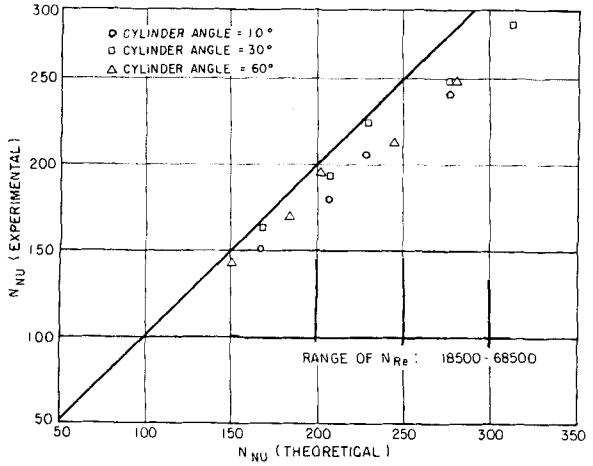

Fig. 7. Comparison of experimental and theoretical heat transfer rates for water.

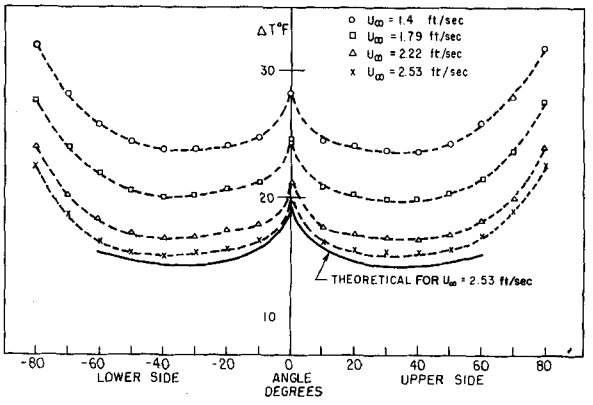

Fig. 9. Temperature distribution around the cylinder. Solution 0.35% carboxymethylcellulose 70.

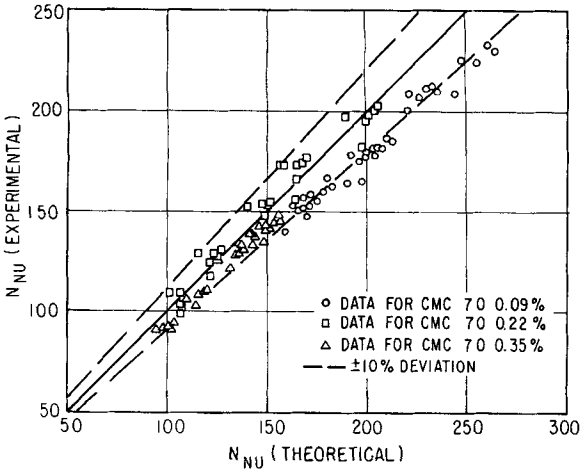

Fig. 10. Comparison between experimental and theoretical heat transfer rates for carboxymethylcellulose solutions.

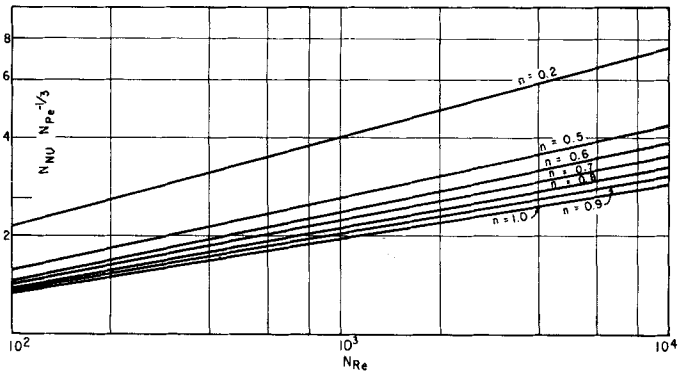

Fig. 12. Local heat transfer rates to pseudoplastic fluids from a cylinder at an angle of 10 deg. from the forward stagnation point.

the maximum variation in the center of the tunnel, at the higher Reynolds numbers, was less than 5%. The central 4-in. section appears indeed to contain a rather uniform velocity distribution with minimum three-dimensional effects and was used therefore for the heat transfer experiments on the cylinder.

The rheological data for the three carboxymethylcellulose solutions are presented in Table 2. For the 0.22% carboxymethylcellulose and the 0.35% one especially the rheological properties were determined for a wide range of shear rates with both carbon tetrachloride and mercury manometers, in order to verify the applicability of the power law to such systems. It was observed however that the measurements could best be fitted by two straight lines over two different ranges of shear rate rather than by only one for the entire range indicated in Table 2. This means that for those carboxymethylcellulose solutions the parameters K and n are not constant over the entire range of the measured shear rates and that the range of shear rate at the surface of the cylinder must be determined before the proper values of the rheological parameters can be used.

The carboxymethylcellulose solutions were also tested by standard techniques to ascertain whether or not they exhibited any viscoelasticity, thixotropy, or the Weissenberg effect (*13*), but it was quickly realized that to all appearances these complicating factors were fortunately absent.

A typical pressure distribution over the 2-in. aluminum cylinder for the 0.22% carboxymethylcellulose 70 solution is shown in Figure 6 for different velocities, together with the pressure profile with water at a Reynolds number of 48,000 and the expression predicted from potential flow theory (*12*) if the characteristic velocity is set equal to $2U_\infty$:

$$\frac{\Delta P}{1/2\,\rho\,U_\infty^2} = 1 - 4\Phi^2(x) = 1 - 4\sin^2 x_1 \qquad (14)$$

It is seen that in the region from 0 to 60 deg. the pressure distribution for water and the carboxymethylcellulose solutions had a negligible difference, and that the shape of the pressure distribution curve was not affected by variations in the Reynolds number. It can be concluded then that for laminar flow the pressure profile in this region is unaffected by either the rheological properties of the carboxymethylcellulose solutions or the velocity of the fluid. It is also believed that the rather good agreement between the experimental data and Equation (14) up to an angle of 60 deg., as measured from the forward stagnation point, is probably due to the presence of wall effects. Beyond 60 deg. the data deviate sharply from Equation (14), and the pressure minima indicate that, as with Newtonian fluids, the separation point occurs at around 80 deg.

The experimental pressure distribution curve shown in Figure 6 was used to express $\Phi(x_1)$ in the form of a polynomial, $ax_1 - bx_1^3$, where the coefficients a and b equal to 0.92 and 0.131, respectively, were determined by a least-squares method. This polynomial was then substituted in Equation (13), and the theoretical surface temperature distribution was finally calculated from Equation (11).

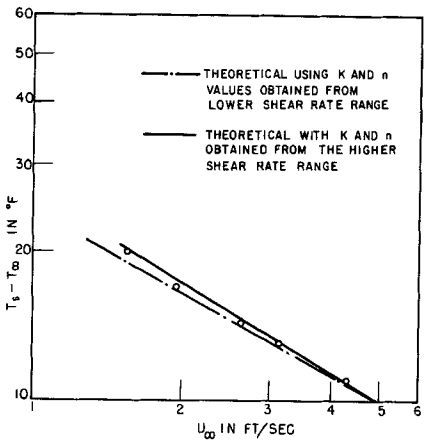

Fig. 11. Experimental and theoretical temperature values at an angle of 10 deg. on the cylinder for 0.22% carboxymethylcellulose.

HEAT TRANSFER MEASUREMENTS

Heat transfer measurements were first carried out with water to confirm the proper functioning of all parts of the equipment, and the experimentally obtained local Nusselt numbers are compared with the theoretically calculated values in Figure 7. The theoretical N_{Nu} was in all cases greater with a maximum deviation of about 14%, but in view of the segmented heating of the cylinder this discrepancy was expected and the performance of the experimental assembly was therefore considered satisfactory.

The experiments were then continued with the carboxymethylcellulose solutions, and the results are presented in Figures 8 and 9, where ΔT has been plotted vs. the angle for different Reynolds numbers, and in Figure 10, where all the experimentally determined Nusselt numbers for the three different carboxymethylcellulose solutions have been compared with the theoretically calculated predictions. The generalized Prandtl number N_{Pr} for all three solutions was large (order of magnitude 100), which insured the applicability of the $N_{Pr} >> 1$ approximation. The measurements for the 0.09% carboxymethylcellulose were however not quite as accurate as for the other two solutions, since it was discovered that the uncertainties in the values of U_∞ were somewhat larger. In the plots of ΔT vs. angle it is observed that the shapes of the theoretical and the experimental curves do agree quite well and that, although the infinite temperature at the stagnation point as predicted by Equations (11) to (13) with $\Phi(x_1) = x_1$ cannot be physically realized, the experimen-

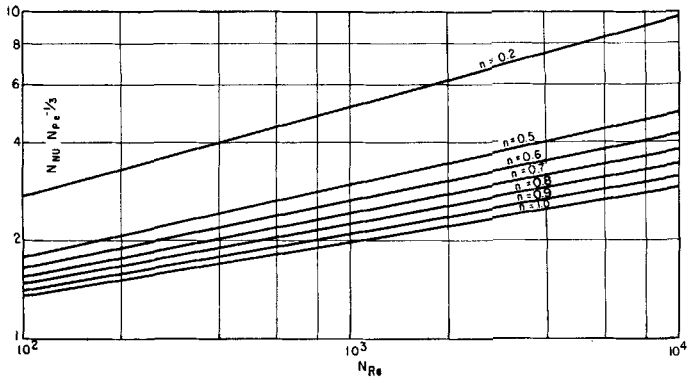

Fig. 13. Local heat transfer rates to pseudoplastic fluids from a cylinder at an angle of 30 deg. from the forward stagnation point.

tal data do indeed show a sharp rise in temperature as the stagnation point is approached. (Incidentally it can easily be shown (*11*) that the boundary layer equations cannot hold near the stagnation point no matter how large N_{Re} is, and that the theoretical prediction of an infinite temperature at that point must therefore be ignored.) The comparison between theory and experiment was carried out only up to an angle of 60 deg. since, as the separation point (80 deg.) was approached, temperature fluctuations set in which invalidated the theoretical predictions.

Finally it is seen from Figure 10 that the experimentally determined N_{Nu} does follow the theoretical values rather well, especially since the 10% discrepancy can to a large extent be attributed to the nonuniformity of the heat flux and to the slight uncertainty in the determination of U_∞.

Before any conclusions are drawn as to the success of the boundary layer theory in non-Newtonian fluids, it will undoubtedly be of value to point out what effect experimental inaccuracies in measuring the temperature, the rheological parameters, the free stream velocity, and the pressure profile could have on the theoretically calculated surface temperature distribution, and to ascertain how the experimental results would be influenced by the variable fluid properties, which throughout the theoretical analysis were assumed constant.

In order to determine the uncertainty introduced by the assumption of constant properties, a set of experiments were performed with three different values of Q which covered a threefold range. The measurements were repeated at three different angles and at constant flow conditions. It was found that within the available experimental accuracy $\Delta T/Q$ was independent of Q for all three angles, thus indicating that the effect of variation of fluid properties in the thermal boundary layer was unimportant, at least for temperature differences ΔT of the order of 25°F. It was also established by a theoretical analysis that under the conditions of all the experiments the contribution to the energy equation of the mechanical dissipation function inside the boundary layer was negligible since, in the absence of any direct surface heating, it could bring about a rise in the surface temperature of the cylinder of only about 0.1°F.

The temperature drop between the back of the Nichrome strip and its front face was calculated approximately from the conduction equations and found to be 0.018 ΔT.

The accuracy of the potentiometer assembly for the temperature measurements was of the order of 0.2°F. which amounted to about ½ to 1½% of the values of ΔT. Q was recorded by means of the voltmeter and the ammeter with an accuracy of more than 1%.

The deviations between the adjacent thermocouple readings on the strip were caused by the surface roughness of the cylinder and the possible three-dimensional flow disturbances caused by the nonuniformity of the fluid velocity across the test section. The surface roughness was of the order of ± 0.003 in. and was likely to cause disturbances in the thermal boundary layer in view of its small dimensions and bring about differences in the thermocouple measurements. Similarly if the velocity in the test section was not maintained uniform, significant differences in thermocouple readings were recorded.

The errors in the velocity measurements could not unfortunately be maintained lower than ± 5%, especially at the very low flow rates. This was due to inherent inaccuracies in the differential manometer readings caused by the presence of the carboxymethylcellulose solutions, the gel centers of which seemed to support a shear stress in the pitot tube (*3a*). The bleeding technique described earlier overcame this difficulty to a large extent if care was taken to push all the carboxymethylcellulose solutions out of the pitot tube, but the error in the velocity measurements could not be eliminated altogether.

In the theoretical calculations for the two carboxymethylcellulose solutions (0.22% and 0.35%) the computed shear rate at the surface of the cylinder at different angles indicated that for velocities less than 2 ft./sec. the shear rate at 10 and 20 deg. fell in the lower range of the rheological curves. Fortunately however for both these fluids the value of $N_{Re}^{\frac{1}{1+n}}$ (and therefore the value of ΔT and N_{Nu}) did not change more than 3 to 4% in the range investigated when the set of values of K and n was changed from one shear rate range to another. This is clearly brought out in Figure 11, where ΔT is plotted vs. U_∞ at 10 deg. for the 0.22% carboxymethylcellulose with both sets of rheological constants. The two theoretical functions are shown here, and since they differ by only a small amount, either of the two sets could have been used under these rather special circumstances.

Thus with the use of the boundary-layer theory and the asymptotic form of the energy equation for $N_{Pr} >> 1$, it has been possible to predict the local rate of heat transfer from a cylinder to power-law non-Newtonian fluids in forced convection flows. The agree-

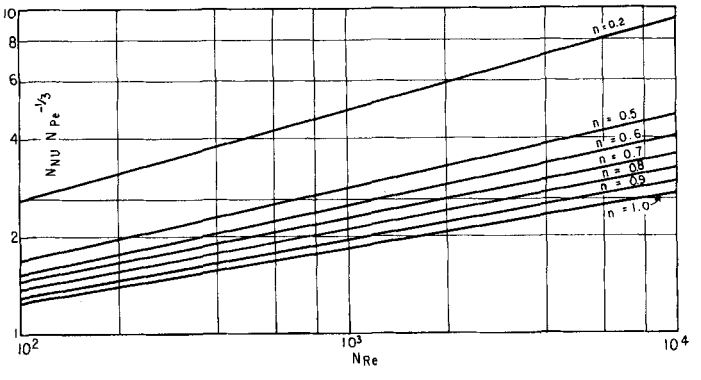

Fig. 14. Local heat transfer rates to pseudoplastic fluids from a cylinder at an angle of 60 deg. from the forward stagnation point.

ment between the theoretical calculations and the experimental measurements is indeed excellent in the region of the cylinder where the boundary-layer equations apply (beyond 60-deg. the theoretical calculations will not be too accurate because of the proximity of the separation point). It now remains to determine the value of n at which for heat transfer purposes it becomes necessary to take the non-Newtonian behavior of the fluid into account. At first glance this comparison between a non-Newtonian substance and an equivalent Newtonian one would naturally appear to be somewhat questionable, since one must remember that the power-law fluids have two rheological parameters in place of the Newtonian viscosity coefficient, and that in Equation (3) the units of K depend on the value of n. Thus the definition of the dimensionless groups generally used for correlating heat transfer data in Newtonian fluids had to be extended. In this manner a generalized Reynolds number was derived for one-dimensional flow systems, and a generalized Prandtl number emerged from the dimensionless form of the boundary-layer energy equation. The generalized Prandtl number thus obtained is however not only dependent upon the properties of the fluid (as for a Newtonian substance), but is a function also of the velocity and the characteristic length of the surface. In an attempt therefore to compare the heat transfer rates of systems with different rheological properties one is clearly confronted with an additional difficulty.

Fortunately the form of Equation (11) suggests that if the heat transfer results were plotted with $N_{Nu}N_{Pe}^{-1/3}$ as the ordinate and N_{Re} as the abscissa, this difficulty would be eliminated. This is so because the ordinate would in such a case be independent of n and K, which would not be true in the $N_{Nu}N_{Pr}^{-1/3}$ vs. N_{Re} plot commonly used for heat transfer correlations.

In Figures 12 to 14 the theoretical heat transfer expressions are presented in the form of $N_{Nu}N_{Pe}^{-1/3}$ vs. N_{Re} plots for different positions of the cylinder surface. Lines are shown for values of n ranging from 0.2 to 1. One can see that the deviations from Newtonian behavior increase as n decreases, and also that with increasing x_1 and N_{Re} the difference in the Nusselt number from the corresponding Newtonian value also increases. Although it is true that for values of n between 0.8 and 1.0 one may assume Newtonian behavior and set K equal to the viscosity μ without introducing any significant errors, it is obvious that for $n < 0.8$ the Nusselt number will differ appreciably from its correct value, if calculated on the basis of a Newtonian theory. In particular large errors will be incurred if the Newtonian assumption is made when $n = 0.2$ or lower. It may be stated then that the necessity of taking the non-Newtonian behavior into consideration depends on the extent of accuracy desired in heat transfer calculations as well as the value of n. Thus for example for clay suspensions where n is of the order of 0.2 to 0.3 (7), even a rough calculation of heat transfer rates will necessitate the consideration of the non-Newtonian property of the fluid.

One can conclude then that the boundary-layer theory has been successfully extended to include heat transfer to power-law non-Newtonian fluids, and that the experimental heat transfer results for the flow past a cylinder were shown to agree with the theoretical predictions which were based on an asymptotic expression for N_{Nu}, derived for large N_{Pr}. It was found that for the flow past a cylinder the experimental measurements of the local rate of heat transfer were in complete agreement with the theoretical calculations up to an angle of 60 deg. from the forward stagnation point, and that for heat transfer purposes fluids with $n < 0.8$ show significant deviations from Newtonian behavior.

ACKNOWLEDGMENT

This work was supported in part by a grant from the National Science Foundation and a grant from the Petroleum Research Fund administered by the American Chemical Society. Grateful acknowledgment is made to the donors of these funds.

NOTATION

A = surface area
c_p = specific heat
D = diameter of capillary
g_n = function of n given numerically in Table 1.
k = thermal conductivity
K, n = parameters in the power-law model, Equation (3)
L = a characteristic length (for the cylinder, L = the radius)
N_{Nu} = the Nusselt number; $N_{Nu} = \frac{QL}{Ak}\frac{1}{T_s - T_\infty}$
N_{Pe} = the Peclet number; $N_{Pe} = \frac{c_p \rho U_\infty L}{k}$
N_{Pr} = the Prandtl number; $N_{Pr} = \frac{c_p U_\infty \rho L}{k(N_{Re})^{\frac{2}{1+n}}}$
N_{Re} = the Reynolds number; $N_{Re} = \frac{\rho U_\infty^{2-n} L^n}{k}$
Q = rate of heat transferred, in B.t.u./hr.
T = temperature
T_s = temperature of the surface
T_∞ = temperature of the bulk of the fluid
$U_i(x)$ = velocity component outside the boundary layer
U_c = characteristic velocity (for the cylinder, $U_c = 2\,U_\infty$)
U_∞ = velocity of the free stream
u = velocity component along x ($u_1 = u/U_c$)
V = average velocity in the capillary $\left(V = \frac{\text{flow rate}}{\pi(D/2)^2}\right)$
v = velocity component along y $\left(v_1 = N_{Re}^{\frac{1}{1+n}}\frac{v}{U_c}\right)$
x = distance along the surface from the leading edge ($x_1 = x/L$)
y = distance normal to the surface $\left(y_1 = N_{Re}^{\frac{1}{1+n}}\frac{y}{L}\right)$

Greek Letters

ΔT = $T_s - T_\infty$
Γ = the gamma function
ρ = density
τ = the shear stress
Φ = U_i/U_c
λ = $(\partial u_1/\partial y_1)_{y1=0}$

LITERATURE CITED

1. Acrivos, Andreas, *J. Aeronaut. Space Sci.*, **27**, 314 (1960).
2. ———, M. J. Shah, and E. E. Petersen, *A.I.Ch.E. Journal*, **6**, 410 (1960).
3. Acrivos, Andreas, *Physics of Fluids*, **3**, 657 (1960).

3a. De Butts, E., J. Hudy, and J. Elliott, *Ind. Eng. Chem.*, **49**, 94 (1957).

4. Kiser, K. M., Ph.D. thesis, Johns Hopkins University, Baltimore, Maryland (1956).
5. Lighthill, M. J., *Proc. Roy. Soc. (London)*, **A202**, 359 (1950).
6. Merrington, A. C., *Nature*, **152**, 663 (1943).
7. Metzner, A. B., "Advances in Chemical Engineering," T. B. Drew and J. W. Hoopes, Jr., ed., Vol. 1, pp. 79-150, Academic Press, New York (1956).
8. Morgan, G. W., and H. H. Warner, *J. Aeronaut. Sci.*, **23**, 937 (1956).
9. Oldroyd, J. G., *Proc. Roy. Soc.*, **A245**, 291 (1958).
10. Rivlin, R. S., *ibid.*, **A193**, 260 (1948); Rivlin, R. S., and J. L. Ericksen, *J. Rat. Mech. and Anal.*, **4**, 323 (1945).
11. Shah, M. J., Ph.D. thesis, Univ. California, Berkeley, California (1961).
12. Schlichting, H., "Boundary Layer Theory," McGraw-Hill, New York (1955).
13. Wilkinson, W. L., "Non-Newtonian Fluids," Pergamon Press, New York (1960).
14. Whittaker, E. T., and G. Robinson, "The Calculus of Observation," Blackie and Sons, London, England (1944).

Manuscript received August 15, 1961; revision received January 21, 1962; paper accepted February 21, 1962. Paper presented at A.I.Ch.E. New York meeting.